Inorganic Chemistry

Article

pubs.acs.org/IC

Construction of a Polyhedral Metal−Organic Framework via a Flexible Octacarboxylate Ligand for Gas Adsorption and Separation

Zu-Jin Lin,[†] Yuan-Biao Huang,[†] Tian-Fu Liu,[†] Xiang-Ying Li,[†,‡] and Rong Cao*[,†]

[†]State Key Laboratory of Structural Chemistry, Fujian Institute of Research on the Structure of Matter, Chinese Academy of Sciences, Fuzhou 350002, P. R. China

[‡]Gradutate School of the Chinese Academy of Sciences, Beijing 100039, P. R. China

Supporting Information

ABSTRACT: A flexible octacarboxylate ligand, tetrakis[(3,5-dicarboxyphenyl)oxamethyl]methane (H_8X), has been used to construct a highly porous metal−organic framework $(In_2X)(Me_2NH_2)_2(DMF)_9(H_2O)_5$ (**1**), which is comprised of octahedral and cuboctahedral cages and shows a rare (4,8)-connected scu topology. Gas adsorption studies of N_2, H_2 on the actived **1** at 77 K reveal a Langmuir surface area of 1707 m^2 g^{-1}, a BET surface area of 1555 m^2 g^{-1}, a total pore volume of 0.62 cm^3 g^{-1}, and a H_2 uptake of 1.49 wt % at 1 bar and 3.05 wt % at 16 bar. CO_2, CH_4, and N_2 adsorption studies at 195, 273, 285, and 298 K and also ideal adsorbed solution theory (IAST) calculations demonstrate that **1** has high selectivites of CO_2 over CH_4 and N_2. The resulting framework represents a MOF with the highest gas uptakes and gas selectivities (CO_2 over CH_4 and N_2) constructed by flexible ligands.

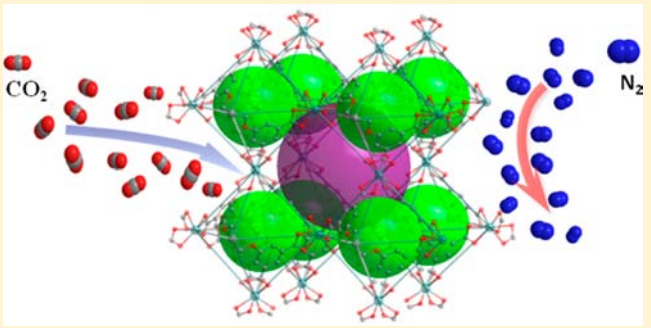

INTRODUCTION

Microporous metal−organic frameworks (MOFs) have received considerable attention because of their intriguing topologies and potential applications as functional materials.[1] Thus far, by judicious selection of the metal cations (or clusters) and rigid organic linkers with fixed geometry, a large number of porous MOFs have been assembled with predesigned structural topology, and the typical example is employing a series of dendritic hexacarboxylate ligands and paddle-wheel secondary building blocks (SBUs) to construct highly porous isoreticular frameworks (such as PCN-61, PCN-66, PCN-68,[2] NOTT-112,[3] and NU-100[4]) with rht topology. Unlike rigid aromatic ligands, flexible ligands can adjust their configurations properly to meet the geometric requirement of the central metal atoms/clusters, which results in a variety of fascinating and multifunctional MOFs.[5] Actually, even for a fixed chemical composition, supramolecular isomerism is a common phenomenon during the assembly process via flexible ligands.[6] Obviously, it is a good opportunity for developing novel functional materials and a better understanding of self-assembly and crystal growth by utilization of the flexible linkers.

Recently, we have been interested in the use of flexible multicarboxylate linkers, such as tetrakis[4-(carboxyphenyl)-oxamethyl]methane,[7] 5-(3,5-dicarboxybenzyloxy)-isophthalic acid,[8] tetrakis[(3,5-dicarboxyphenoxy)methyl]methane) (H_8X),[9] and 1,3,5-tris[3-(carboxyphenyl)oxamethyl]-2,4,6-trimethylbenzene,[10] to construct porous functional MOFs and promote investigation of the structure−property relationship. For example, we synthesized a highly porous MOF $(In_2X)(Me_2NH_2)_2(DMA)_5(H_2O)_2$ via the flexible ligand H_8X and elucidated how the guest molecules (tetraalkyammonium cations) determine the porosities and tune the gas sorption properties of the framework.[11] Replacing dimethylacetamide (DMA) solvents with dimethylformide (DMF) in the starting materials, we successfully isolated another supramolecular isomer $(In_2X)(Me_2NH_2)_2(DMF)_9(H_2O)_5$ (**1**) under the same solvothemal conditions. Herein, we report the synthesis, X-ray structure, and gas sorption properties of the highly porous framework **1** based on the flexible octacarboxylate ligand (H_8X, Scheme 1). Structural analysis reveals that the framework is built by octahedral and cuboctahedral cages. Gas adsorption measurements demonstrate that the material has a large surface

Scheme 1. Structure of Tetrakis[(3,5-dicarboxyphenoxy)methyl]methane), H_8X

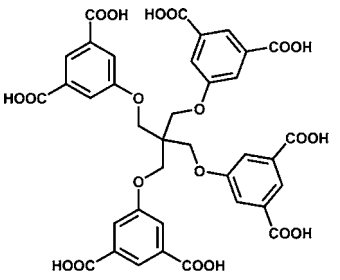

Received: November 26, 2012
Published: March 7, 2013

   dx.doi.org/10.1021/ic302583a | *Inorg. Chem.* 2013, 52, 3127−3132

area and good H_2 and CO_2 storage capacity. Ideal adsorbed solution theory (IAST) calculations predict the material shows high selectivites of CO_2 over CH_4 and N_2 at room temperature.

EXPERIMENTAL SECTION

Materials and General Methods. All chemicals and solvents purchased were of analytical grade and used without further purification. Ligand H_8X was synthesized according to the literature.[11] Elemental analyses (C, H, and N) were carried out on an Elementar Vario EL III analyzer. Infrared (IR) spectra were recorded on a PerkinElmer Spectrum One as KBr pellets in the range 4000−400 cm^{-1}. ^1H NMR spectra wererecorded at ambient temperature on a BRUKER AVANCE III spectrometer (Figure S1, Supporting Information); chemical shifts were referenced to TMS in the solvent signal in d_6-DMSO. Powder X-ray diffraction (PXRD) data were collected on a Rigaku MiniFlex2 diffractometer working with Cu Kα radiation, and the recording speed was 5° min^{-1} over the 2θ range of 5−50° at room temperature (Figure S2, Supporting Information). Thermogravimetric analyses (TGA) were performed under a nitrogen atmosphere with a heating rate of 10 °C/min using an SDT Q600 thermogravimetric analyzer (Figure S3, Supporting Information). Supercritical carbon dioxide (SCD) drying was performed with SFT-10 pump linkup pressure vessel and the Rxtrol Jr reactor temperature control system. The simulated powder pattern was calculated using Mercury 2.0. Purity and homogeneity of the bulk product were determined by comparison of the simulated and experimental X-ray powder diffraction patterns.

Synthesis of $(In_2X)(Me_2NH_2)_2(DMF)_9(H_2O)_5$ (1). A sample of $InCl_3{\cdot}4H_2O$ (0.05 mmol, 15 mg), H_8X (0.025 mmol, 20 mg), and DMF (4 mL) was mixed in 23 mL Teflon-lined stainless steel vessel. The mixture was heated under autogenous pressure at 120 °C for 72 h and then cooled to room temperature at a constant rate of 0.05 °C/min. Colorless block crystals suitable for X-ray crystal analysis were obtained by filtration, washed several times with DMF, and dried in air at ambient temperature. The compound is stable in air and insoluble in common organic solvents such as methanol, ethanol, acetonitrile, acetone, DMSO, and DMF. Yield: 75% (based on H_8X). Anal. Calcd for $C_{68}H_{57}In_2N_{11}O_{34}$: C, 45.33; H, 3.19; N, 8.55. Found: C, 45.26; H, 3.10; N, 8.56. IR (KBr): ν = 3399 (br), 3085 (m), 1660 (s), 1565 (s), 1446 (m), 1371 (s), 1252 (m), 1038 (m), 922 (w), 840 (m), 783 (m), 733 (m), 560 (m).

Single-Crystal X-ray Crystallography. Crystal diffraction data of compound **1** was collected on a Rigaku Saturn 724+ diffractometer equipped with graphite-monochromatized Mo Kα radiation (λ = 0.71073 Å) and a CCD area detector at room temperature. Absorption correction was performed using the CrystalClear program.[12] Structure was solved by direct methods and refined by full matrix least-squares on F^2 using the SHELXTL-97 program package.[13] All non-hydrogen atoms were refined with anisotropic displacement parameters. Positions of hydrogen atoms attached to carbon atoms were generated geometrically. Attempts to locate and model the highly disordered solvent molecules and counterions in the pores were unsuccessful. Therefore, the SQUEEZE routine of PLATON was used to remove the diffraction contribution from these solvents to produce a set of solvent-free diffraction intensities.[14] Details of the structure solution and final refinements for **1** are given in Table S2, Supporting Information. CCDC 908192 contains the crystallographic data for this paper. Data can be obtained from the Cambridge Crystallographic Date Center via www.ccdc.cam.ac.uk.

Gas Sorption Measurements. Low-pressure gas (nitrogen, methane, carbon dioxide, and hydrogen) adsorption measurements were carried out on an ASAP (Accelerated Surface Area and Porosimetry) 2020 System. High-pressure hydrogen and methane adsorption measurements were carried out on an Intelligent Gravimetric Sorption Analyzer IGA100B instrument. Sample was actived by the supercritical carbon dioxide (SCD) method (the SCD drying was performed with a SFT-10 pump linkup pressure vessel and the Rxtrol Jr reactor temperature control system). After removal of solvents by SCD drying, sample was dried under a dynamic vacuum ($<10^{-3}$ Torr) at 313 K for 10 h. Before gas adsorption measurement, sample was dried again using the "outgas" function of the surface area analyzer for 5 h at 313 K. Measurements were maintained at 77, 87, 195, 273, 285, and 298 K with a liquid nitrogen bath, a liquid argon bath, an acetone−dry ice bath, an ice−water bath, a water-bath, and a water-bath, respectively.

RESULT AND DISSCUSION

Crystals of **1** were obtained under solvothemal conditions by mixing H_8X and $InCl_3{\cdot}4H_2O$ in a 1:2 molar ratio in dimethylformide at 120 °C for 3 days. The phase purity of the bulk product was confirmed by powder X-ray diffraction (PXRD) (Figure S2, Supporting Information). Single-crystal X-ray diffraction analysis reveals that compound **1** crystallizes in the orthorhombic space group $P222_1$. As shown in Figure S4, Supporting Information, the asymmetric unit of **1** contains an X^{8-} ligand and two In(III) cations locating in the C_2 axes. In the structure, each In(III) center is eight coordinate, binding to eight oxygen atoms from four carboxylate groups but serves as a 4-connected node due to the carboxylate groups adopting a bidentate chelating coordination mode. Each X^{8-} ligand binds to eight separate In(III) centers, acting as a 8-connected cubic node, and as expected, the anionic framework shows a rare 3D (4,8)-connected network with scu topology.[15]

The structure of **1** can be viewed as the alternate packing of two types of cages (cages A and B) in 3D space. Both the In(III) center and the quaternary carbon atom from the X^{8-} ligand participate in construction of these two cages. In cage A (Figure 1a), four In(III) centers acting as four octahedral

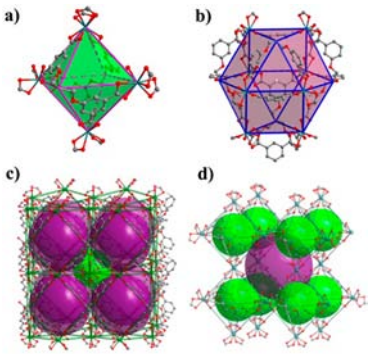

Figure 1. View of (a) cage A, (b) cage B, (c) cage A surrounded by eight B cages, and (d) cage B also surrounded by eight A cages.

vertices arrange in a square plane (In_4 plane) and two central sp^3 carbon atoms from two X^{8-} ligands serving as other two octahedral vertices locate in and out the In_4 square plane. Cage B (Figure 1b) is a distorted cuboctahedron. In cage B, eight In(III) centers and four quaternary carbon atoms from four X^{8-} ligands act as 12 vertices of the cuboctahedron. The approximate diameter of the inner sphere of cages A and B are 8.2 and 13.0 Å, respectively. In the structure, each cage A is surrounded by eight B cages and each cage B is also encompassed by eight A cages via sharing the triangular faces (Figure 1c and 1d). Thus, the structure of **1** can be seen as that cages A occupy the octahedral space, forming by simple cubic packing of B cages.

Compound **1** possesses three types of 1D square channels with dimension of about 9.3 Å along the crystallographic *a*, *b*, and *c* axes, which are interconnected with each other (Figure S5, Supporting Information). The potential free volume of **1** is

dx.doi.org/10.1021/ic302583a | Inorg. Chem. 2013, 52, 3127−3132

65.1% as calculated by PLATON (1.8 Å probe radius) after removal of guest solvent molecules, and the pore volume is 0.87 $cm^3\ g^{-1}$. The permanent porosity of the actived sample was confirmed by the N_2 sorption experiment at 77 K. As shown in Figure 2, the fully activated sample reveals a reversible typical

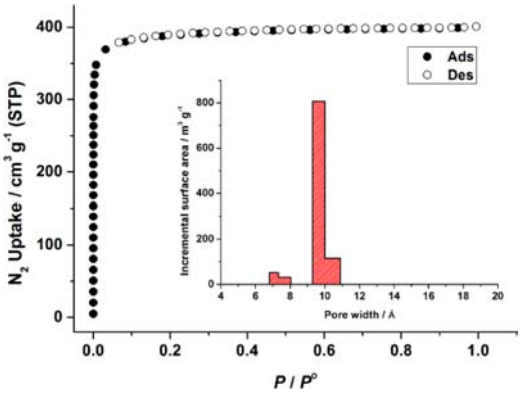

Figure 2. Experimental N_2 isotherm at 77 K for **1**; filled and open symbols represent adsorption (Ads) and desorption (Des) data, respectively. (Inset) Pore size distribution (PSD) calculated by density functional theory (DFT).

type-I behavior as expected for microporous materials, which is coincidental with the crystal structure. Derived from N_2 adsorption, the Langmuir surface area of **1** is 1707 $m^2\ g^{-1}$, corresponding to a BET surface area of 1555 $m^2\ g^{-1}$. The BET surface area is among the highest MOFs constructed by flexible ligands (Figure 3).[16] A pore distribution analysis by density functional theory (DFT) shows that there is a narrow distribution of micropores at around 6.7 and 9.3 Å, corresponding to the diameters of cage A and cage B, albeit those values are smaller than that derived from the single-crystal structure. The pore volume estimated by *t*-plot analysis is 0.62 $cm^3\ g^{-1}$, which is also a little smaller than the value (0.87 $cm^3\ g^{-1}$) calculated from the structure. The results can be explained that the disorder counterions $(CH_3)_2NH_2^+$ occupy in the channels, decreasing the void of the channels.

The high porosity and surface area of **1** prompted us to evaluate its hydrogen adsorption performances. The low-pressure hydrogen sorption isotherm of the desolvated sample at 77 K reveals reversible hydrogen adsorption as presented in Figure 4. The excess gravimetric hydrogen uptake capacity of **1** reaches 1.49 wt % at 1 bar, comparable to MOF-5, MOF-74,[17] and CUK-1,[18] and is among the highest for MOFs with flexible

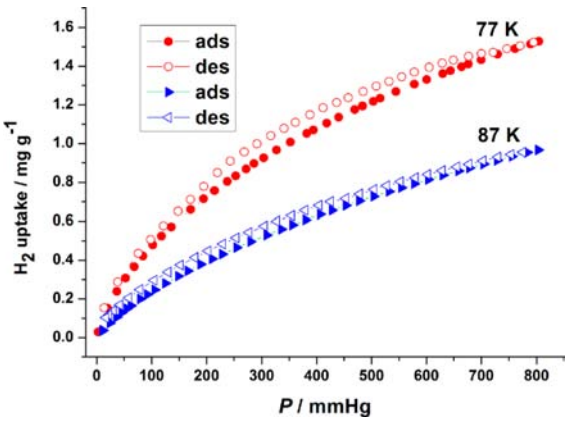

Figure 4. Experimental H_2 isotherms at 77 and 87 K for **1**.

ligands (Figure 3a).[7a,19] The sample exhibits an increasing hydrogen uptake accompanied with the increasing pressure and excess gravimetric value reaching 3.05 wt % at 77 K and 16 bar, which is comparable to that of MIL-53(Cr) (3.1 wt %) under the same measurement conditions.[20] At 77 K, the maximum excess hydrogen uptake value is 3.21 wt % at around 30 bar, corresponding to the total hydrogen uptake is 4.26 wt % (Figure 5). To evaluate the heats of adsorption (Q_{st}) for H_2 in

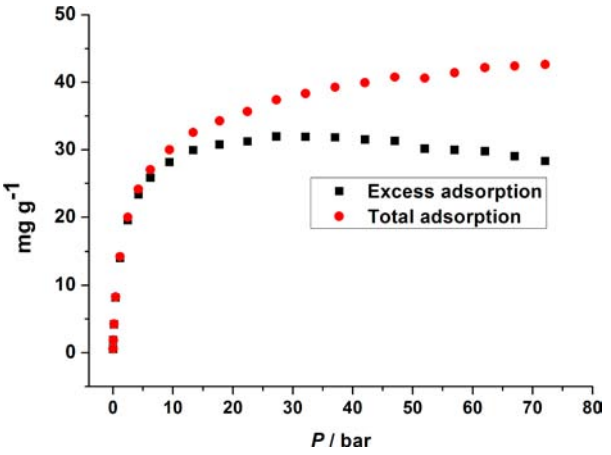

Figure 5. High-pressure H_2 adsorption isotherm for **1** at 77 K.

compound **1**, H_2 adsorption isotherms were also measured at 87 K. Adsorption data were fitted using the virial-type expression, and the heats of adsorption were calculated using

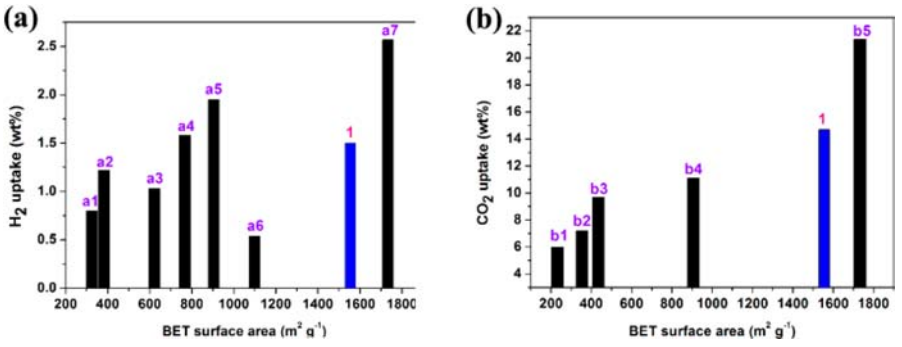

Figure 3. Comparison of reported MOFs via flexible ligands: (a) BET surface area and H_2 uptake at 77 K and 1 bar; (b) BET surface area and CO_2 uptake at 298 K and 1 bar (Table S1, Supporting Information).

dx.doi.org/10.1021/ic302583a | *Inorg. Chem.* 2013, 52, 3127−3132

virial coefficients. As shown in Figure 6, the initial hydrogen adsorption enthalpy is 6.15 kJ mol^{-1}. With the increase in H_2 coverage, Q_{st} of **1** decreases steadily.

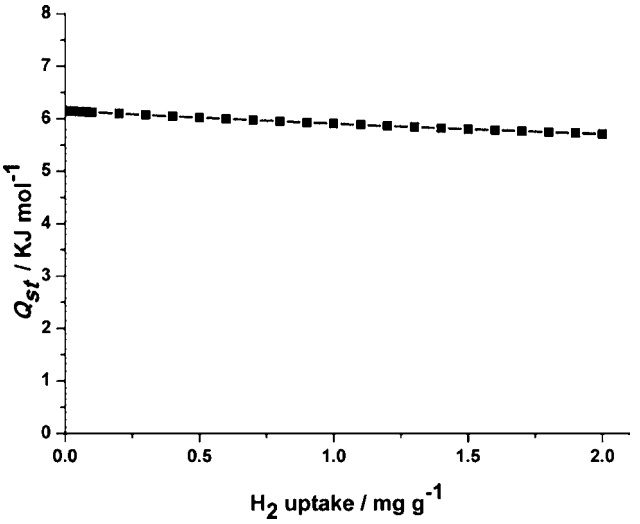

Figure 6. Isosteric heats of H_2 adsorption for **1**.

To further investigate the gas sorption properties of **1**, CO_2, CH_4, and N_2 adsorption measurements have also been carried out, and the results are shown in Figure 7 and summarized in Table 1. At 195 K and 1 bar, compound **1** adsorbs CO_2 up to 370.2 cm^3 g^{-1}, CH_4 up to 202.5 cm^3 g^{-1}, and N_2 up to 43.2 cm^3 g^{-1}. At 273 K and 1 bar, the adsorption capacity for CO_2 is 99.7

Table 1. Comparison of Gas Adsorption Data of 1

			adsorption capacity (cm^3 g^{-1})		
T/K	P/bar	H_2[a]	CO_2	CH_4	N_2
77	1	1.49			401.1
77	16	3.05			
195	1		370.2	202.5	43.2
273	1		99.7	22.5	2.5
285	1		74.6	17.0	
298	1		56.2	13.2	

[a]The unit of hydrogen uptake is wt %.

and 22.5 cm^3 g^{-1} for CH_4 but for N_2 only 2.5 cm^3 g^{-1}. With the increase of temperature to 298 K, the adsorption capacity for CO_2 is 56.2 cm^3 g^{-1} but for CH_4 13.2 cm^3 g^{-1}. CO_2 uptake is among the highest MOFs built by flexible linkers (Figure 3b). Heat of adsorption measurements (Figure 7d) show that compound **1** has an initial affinity of about 21.14 kJ mol^{-1} for CO_2 and 17.45 kJ mol^{-1} for CH_4. The results demonstrate that compound **1** has the ability to selectively adsorb CO_2 over CH_4 and N_2 (Figures 7 and 8a). To further explore the potential properties toward CO_2/CH_4 and CO_2/N_2 gas separation, adsorption selectivities were calculated via ideal adsorption solution theory (IAST) based upon experimental CO_2, CH_4, and N_2 isotherms, and the results are presented in Figure 8b. The adsorption selectivity is defined as $S_{i/j} = (q_1/q_2)/(p_1/p_2)$, where q_i is the amount of i adsorbed and p_i is the partial pressure of i in the mixture. At 1 bar, the predicted CO_2/CH_4 selectivity is 6.40 at 273 K and 5.60 at 298 K (Figure 8b) from equimolar gas-phase mixtures, which is comparable to the high

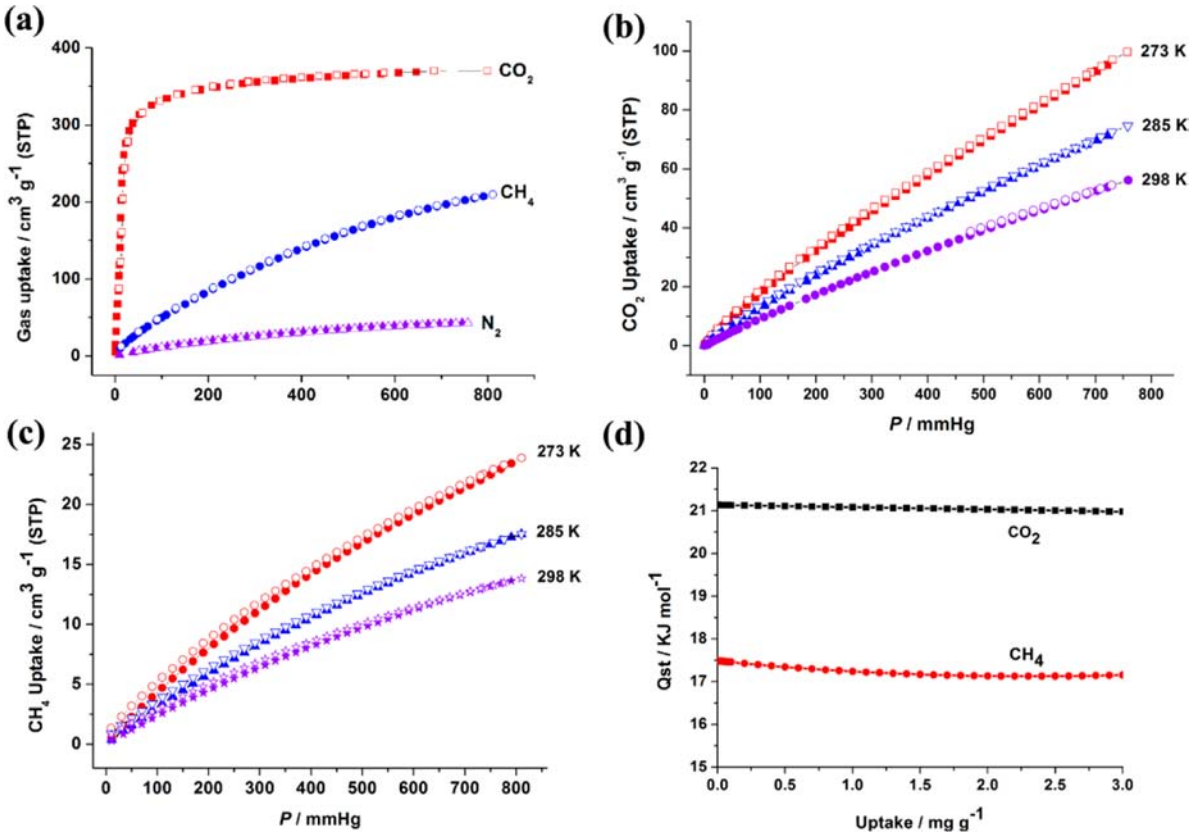

Figure 7. (a) Experimental CO_2, CH_4, and N_2 isotherms at 195 K for **1**. (b) Experimental CO_2 isotherms at 273, 285, and 298 K for **1**. (c) Experimental CH_4 isotherms at 273, 285, and 298 K for **1**. (d) Isoteric heats of CO_2 and CH_4 adsorption for **1**.

dx.doi.org/10.1021/ic302583a | Inorg. Chem. 2013, 52, 3127−3132

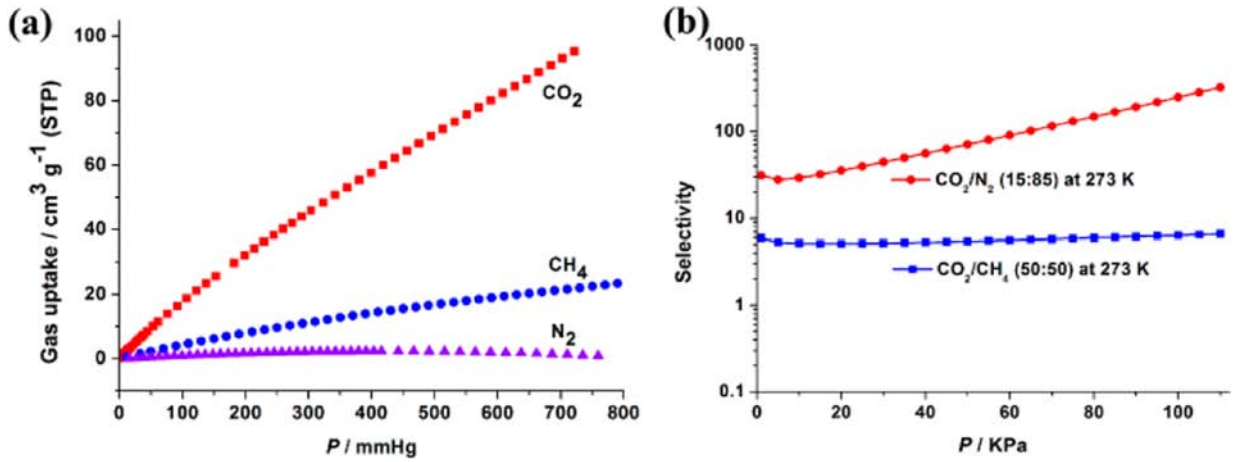

Figure 8. (a) Experimental CO_2, CH_4, and N_2 isotherms at 273 K for **1**. (b) IAST-predicted selectivities for CO_2/CH_4 and CO_2/N_2 adsorption based on observed adsorption isotherms of the pure gas for **1**.

selectivities of CO_2 over CH_4 in reported compounds ZIF-100[21] and HKUST-1.[22] Remarkably, compound **1** shows exceptionally high CO_2/N_2 selectivity at 273 K and 1.0 bar (S = 250.0, CO_2 and N_2 mixtures in a 15:85 molar ratio), which indicates that this material may be a promising adsorbent in the process of CO_2/N_2 separation required for postcombustion CO_2 capture application.

Selective CO_2 adsorption over CH_4 and N_2 in **1** is mainly attributed to the differences in the electrostatic interactions between the porous surface and adsorbates. Recent computational and experimental studies have demonstrated that charged porous framework materials exhibit much stronger binding interactions with CO_2 molecules.[23] Besides, the small kinetic diameter of CO_2 (3.30 Å) enables more adsorbing sites to be accessible in the channel. On the contrary, the larger kinetic diameter of CH_4 (3.80 Å) and N_2 (3.64 Å) makes it difficult for them to diffuse into small cavities.

CONCLUSION

We synthesized a highly porous polyhedral MOF (In_2X)-$(Me_2NH_2)_2(DMF)_9(H_2O)_5$ based on flexible tetrakis[(3,5-dicarboxyphenyl)oxamethyl]methane. Structural analysis reveals that the framework is comprised of octahedral and cuboctahedral cages and shows a rare (4,8)-connected scu topology. After activation by supercritical carbon dioxide (SCD) drying, the material has a large surface area (BET 1555 $m^2\ g^{-1}$) and good H_2 (1.49% at 77 K and 1 bar, 3.05% at 77 K and 16 bar) and CO_2 storage capacity (99.7 $cm^3\ g^{-1}$ at 273 K and 1 bar). Besides, ideal adsorbed solution theory (IAST) calculations predict the material show high selectivites of CO_2 over CH_4 and N_2. The framework presented here represents one of MOFs with highest gas uptakes and gas selectivities (CO_2 from CH_4 and N_2) built by flexible ligands.

ASSOCIATED CONTENT

Supporting Information

Additional structural figures, NMR spectrum, PXRD patterns, TGA curves, derivation of the isosteric heats of adsorption for H_2, CO_2, and CH_4, and crystallographic data for **1**. This material is available free of charge via the Internet at http://pubs.acs.org.

AUTHOR INFORMATION

Corresponding Author

*Phone: +86-591-83796990. Fax: +86-591-83796710. E-mail: rcao@fjirsm.ac.cn. Fax: +86-591-83796710.

Notes

The authors declare no competing financial interest.

ACKNOWLEDGMENTS

This work was financially supported by the 973 Program (2011CB932504, 2012CB821705), NSFC (21221001, 21003128, and 20901078), Fujian Key Laboratory of Nanomaterials (2006L2005), and Key Projects from CAS.

REFERENCES

(1) (a) Sumida, K.; Rogow, D. L.; Mason, J. A.; McDonald, T. M.; Bloch, E. D.; Herm, Z. R.; Bae, T.-H.; Long, J. R. *Chem. Rev.* **2012**, *112*, 724−781. (b) Suh, M. P.; Park, H. J.; Prasad, T. K.; Lim, D.-W. *Chem. Rev.* **2012**, *112*, 782−835. (c) Liu, J.; Thallapally, P. K.; McGrail, B. P.; Brown, D. R.; Liu, J. *Chem. Soc. Rev.* **2012**, *41*, 2308−2322. (d) Zhao, X.; Sun, D.; Yuan, S.; Feng, S.; Cao, R.; Yuan, D.; Wang, S.; Dou, J.; Sun, D. *Inorg. Chem.* **2012**, *51*, 10350−10355. (e) Yang, S.; Lin, X.; Lewis, W.; Suyetin, M.; Bichoutskaia, E.; Parker, J. E.; Tang, C. C.; Allan, D. R.; Rizkallah, P. J.; Hubberstey, P.; Champness, N. R.; Mark Thomas, K.; Blake, A. J.; Schröder, M. *Nat. Mater.* **2012**, *11*, 710−716.

(2) Yuan, D.; Zhao, D.; Sun, D.; Zhou, H.-C. *Angew. Chem., Int. Ed.* **2010**, *49*, 5357−5361.

(3) Yan, Y.; Lin, X.; Yang, S.; Blake, A. J.; Dailly, A.; Champness, N. R.; Hubberstey, P.; Schroder, M. *Chem. Commun.* **2009**, 1025−1027.

(4) Farha, O. K.; Yazaydin, A. O.; Eryazici, I.; Malliakas, C. D.; Hauser, B. G.; Kanatzidis, M. G.; Nguyen, S. T.; Snurr, R. Q.; Hupp, J. T. *Nat. Chem.* **2010**, *2*, 944−948.

(5) (a) Liang, L.-L.; Ren, S.-B.; Zhang, J.; Li, Y.-Z.; Du, H.-B.; You, X.-Z. *Dalton Trans.* **2010**, *39*, 7723−7726. (b) Liang, L.-L.; Zhang, J.; Ren, S.-B.; Ge, G.-W.; Li, Y.-Z.; Du, H.-B.; You, X.-Z. *CrystEngComm* **2010**, *12*, 2008−2010. (c) Zhao, X.; He, H.; Hu, T.; Dai, F.; Sun, D. *Inorg. Chem.* **2009**, *48*, 8057−8059. (d) Sun, J.; Dai, F.; Yuan, W.; Bi, W.; Zhao, X.; Sun, W.; Sun, D. *Angew. Chem., Int. Ed.* **2011**, *50*, 7061−7064. (e) Yan, C.; Li, K.; Wei, S.-C.; Wang, H.-P.; Fu, L.; Pan, M.; Su, C.-Y. *J. Mater. Chem.* **2012**, *22*, 9846−9852. (f) Lan, Y.-Q.; Jiang, H.-L.; Li, S.-L.; Xu, Q. *Inorg. Chem.* **2012**, *51*, 7484−7491.

(6) (a) Kishan, M. R.; Tian, J.; Thallapally, P. K.; Fernandez, C. A.; Dalgarno, S. J.; Warren, J. E.; McGrail, B. P.; Atwood, J. L. *Chem. Commun.* **2010**, *46*, 538−540. (b) Tian, J.; Motkuri, R. K.; Thallapally, P. K.; McGrail, B. P. *Cryst. Growth Des.* **2010**, *10*, 5327−5333.

(7) (a) Guo, Z.; Cao, R.; Wang, X.; Li, H.; Yuan, W.; Wang, G.; Wu, H.; Li, J. *J. Am. Chem. Soc.* **2009**, *131*, 6894−6895. (b) Liu, T.-F.; Lu, J.; Lin, X.; Cao, R. *Chem. Commun.* **2010**, *46*, 8439−8441.
(8) Lin, Z.-J.; Han, L.-W.; Wu, D.-S.; Huang, Y.-B.; Cao, R. *Cryst. Growth Des.* **2013**, *13*, 255−263.
(9) (a) Lin, Z. J.; Liu, T. F.; Xu, B.; Han, L. W.; Huang, Y. B.; Cao, R. *CrystEngComm* **2011**, *13*, 3321−3324. (b) Lin, Z.-J.; Liu, T.-F.; Zhao, X.-L.; Lu, J.; Cao, R. *Cryst. Growth Des.* **2011**, 4284−4287.
(10) lin, Z. J.; lin, X.; Cao, R. *Acta Chim. Sinica* **2012**, *70*, 2012−2015.
(11) Lin, Z.-J.; Liu, T.-F.; Huang, Y.-B.; Lü, J.; Cao, R. *Chem.—Eur. J.* **2012**, *18*, 7896−7902.
(12) Molecular Structure Corporation and Rigaku. *CrystalClear*, Version 1.36; MSC: The Woodlands, TX, and Rigaku Corp.: Tokyo, Japan, 2000.
(13) Sheldrick, G. M. *SHELXS-97, Program for Crystal Structure Solution and Refinement*; University of Göttingen: Göttingen, Germany, 1997.
(14) Spek, A. L., S. A. *Appl. J. Crystallogr.* **2003**, *36*, 7.
(15) (a) Ma, L.; Mihalcik, D. J.; Lin, W. *J. Am. Chem. Soc.* **2009**, *131*, 4610−4612. (b) Mihalcik, D. J.; Zhang, T.; Ma, L.; Lin, W. *Inorg. Chem.* **2012**, *51*, 2503−2508. (c) Tan, C. R.; Yang, S. H.; Champness, N. R.; Lin, X. A.; Blake, A. J.; Lewis, W.; Schroder, M. *Chem. Commun.* **2011**, *47*, 4487−4489.
(16) (a) Kim, T. K.; Suh, M. P. *Chem. Commun.* **2011**, *47*, 4258−4260. (b) Xue, Y.-S.; He, Y.; Ren, S.-B.; Yue, Y.; Zhou, L.; Li, Y.-Z.; Du, H.-B.; You, X.-Z.; Chen, B. *J. Mater. Chem.* **2012**, *22*, 10195−10199.
(17) Rowsell, J. L. C.; Yaghi, O. M. *J. Am. Chem. Soc.* **2006**, *128*, 1304−1315.
(18) Humphrey, S. M.; Chang, J.-S.; Jhung, S. H.; Yoon, J. W.; Wood, P. T. *Angew. Chem., Int. Ed.* **2007**, *46*, 272−275.
(19) (a) Pachfule, P.; Panda, T.; Dey, C.; Banerjee, R. *CrystEngComm* **2010**, *12*, 2381−2389. (b) Zhuang, W.; Ma, S.; Wang, X.-S.; Yuan, D.; Li, J.-R.; Zhao, D.; Zhou, H.-C. *Chem. Commun.* **2010**, *46*, 5223−5225.
(20) (a) Ferey, G.; Latroche, M.; Serre, C.; Millange, F.; Loiseau, T.; Percheron-Guegan, A. *Chem. Commun.* **2003**, 2976−2977. (b) Loiseau, T.; Serre, C.; Huguenard, C.; Fink, G.; Taulelle, F.; Henry, M.; Bataille, T.; Férey, G. *Chem.—Eur. J.* **2004**, *10*, 1373−1382.
(21) Wang, B.; Cote, A. P.; Furukawa, H.; O'Keeffe, M.; Yaghi, O. M. *Nature* **2008**, *453*, 207−211.
(22) Simmons, J. M.; Wu, H.; Zhou, W.; Yildirim, T. *Energy Environ. Sci.* **2011**, *4*, 2177−2185.
(23) (a) Liu, D.; Zhong, C. *J. Mater. Chem.* **2010**, *20*, 10308−10318. (b) Xu, Q.; Liu, D. H.; Yang, Q. Y.; Zhong, C. L.; Mi, J. G. *J. Mater. Chem.* **2010**, *20*, 706−714. (c) Lin, Z.-J.; Yang, Z.; Liu, T.-F.; Huang, Y.-B.; Cao, R. *Inorg. Chem.* **2012**, *51*, 1813−1820.